

Molecular Physics

An International Journal at the Interface Between Chemistry and Physics

ISSN: 0026-8976 (Print) 1362-3028 (Online) Journal homepage: <https://www.tandfonline.com/loi/tmph20>

On the stability and finite-size effects of a columnar phase in single-component systems of hard-rod-like particles

Simone Dussi, Massimiliano Chiappini & Marjolein Dijkstra

To cite this article: Simone Dussi, Massimiliano Chiappini & Marjolein Dijkstra (2018) On the stability and finite-size effects of a columnar phase in single-component systems of hard-rod-like particles, *Molecular Physics*, 116:21-22, 2792-2805, DOI: [10.1080/00268976.2018.1471231](https://doi.org/10.1080/00268976.2018.1471231)

To link to this article: <https://doi.org/10.1080/00268976.2018.1471231>



© 2018 The Author(s). Published by Informa UK Limited, trading as Taylor & Francis Group.



Published online: 15 May 2018.



Submit your article to this journal [↗](#)



Article views: 351



View Crossmark data [↗](#)

On the stability and finite-size effects of a columnar phase in single-component systems of hard-rod-like particles

Simone Dussi^{a,b}, Massimiliano Chiappini^a and Marjolein Dijkstra^{a**}

^aSoft Condensed Matter, Debye Institute for Nanomaterials Science, Utrecht University, Utrecht, The Netherlands; ^bPhysical Chemistry and Soft Matter, Wageningen University, Wageningen, The Netherlands

ABSTRACT

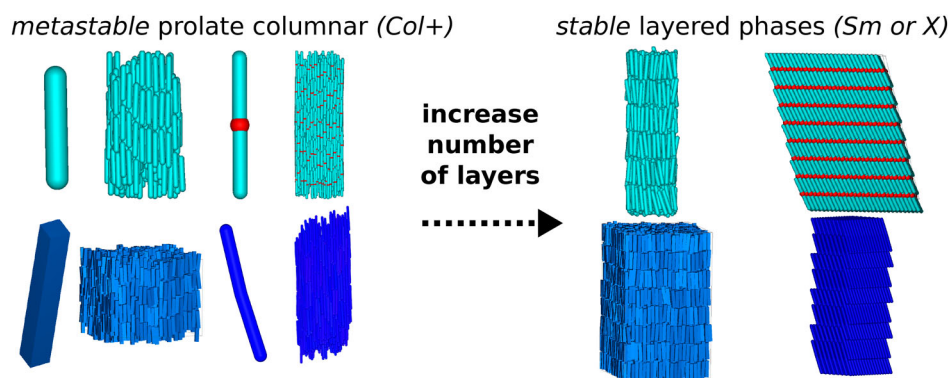
Colloidal rod-like particles self-assemble into a variety of liquid crystal phases. In contrast to the formation of the nematic and smectic phases for which it is well understood that it can be driven by entropy, the stabilisation mechanism of a prolate columnar phase (Col_+), observed for example in fd-virus suspensions, is still unclear. Here, we investigate whether or not a Col_+ phase can exist in a purely entropy-driven single-component system. We perform computer simulations of hard particles with different shapes: spherocylinders, top-shaped rods, cuboidal particles, and crooked rods. We show that the Col_+ phases observed in previous simulation studies are mere artefacts due to either finite-size effects or simulation boxes that are incommensurate with the stable thermodynamic phase. In particular, we observe that the characteristic layering of the stable smectic or crystal phase disappears when the dimension of the simulation box along the direction of the layers is too small. Such a system-size effect depends both on particle shape and the competing phases, and appears to be more pronounced for less anisotropic particles.

ARTICLE HISTORY

Received 26 February 2018
Accepted 16 April 2018

KEYWORDS

Liquid crystals; entropy; columnar phase; hard particles; Monte Carlo simulations




1. Introduction

Moderately dense suspensions of anisotropic colloids can self-assemble into liquid crystal phases, exhibiting long-range orientational order but no, or only partial, positional order [1]. Examples range from organic rods, such as tobacco mosaic viruses, fd-viruses, DNA, to inorganic materials, such as ferric oxyhydroxide rods, boehmite rods, vanadium pentoxide rods and silica rods [2–12]. The different phases can be distinguished on the basis of the microscopic arrangement of the particles. Nematic phases (N) display only long-range orientational order, i.e. the particles are on average aligned along a common

direction; smectic (Sm) phases have an additional 1D positional order, i.e. the particles are arranged in smectic layers; and finally, columnar (Col) phases feature a 2D positional order, i.e. particles form columns that are arranged on a 2D lattice. In the case of biaxial particles, LC phases can be further divided into (i) prolate uniaxial (often denoted with a subscript $+$), (ii) oblate uniaxial (subscript $-$) and (iii) biaxial phases (subscript b), depending on whether the long-range orientational order of the system is associated to (i) the long, (ii) short or (iii) both particle axes. Further classification is possible based on the symmetry of the positional order.

CONTACT Simone Dussi  simone.dussi@wur.nl

**  m.dijkstra@uu.nl

In 1949, Onsager showed in his seminal work that a system of infinitely thin hard rods exhibits a purely entropy-driven phase transition from an isotropic to a nematic phase at sufficiently high densities [13]. Upon increasing the density of the system, the alignment of the rods along a common director becomes favourable at the expense of orientational entropy, but this loss is more than compensated by a gain in translational entropy.

In the 1980s, Frenkel *et al.* employed computer simulations on various hard-particle systems, such as ellipsoids, spherocylinders and disks, to provide evidence for the entropy-driven formation of not only the nematic phase [14] but also the smectic [15] and the columnar phases [16]. Quoting Daan Frenkel from his 1999 review paper: ‘the idea of entropy-driven phase transitions is an old one. However, it has only become clear during the past few years that such phase transformations may not be interesting exceptions, but the rule!’ [17]. Indeed, the number of theoretical and simulation studies on entropy-dominated systems has steadily increased since then [18–27], not only because of their fundamental interest but also due to the concurrent developments in synthesis routes to produce colloidal particles and nanoparticles [28–30]. A large library of differently shaped particles is nowadays available for self-assembly experiments, and in many cases the role of entropy is predominant. For example, silica rods can be considered as a (nearly) perfect experimental realisation of hard spherocylinders, since at sufficiently high salt concentrations the phase behaviour can be mapped onto that of a corresponding hard-particle system, both for a single-component and a binary system [11,12,31]. Suspensions of fd-viruses are another fascinating and widely studied example of colloidal systems composed of rod-like particles [3–5,32–34]. The many competing interactions at different length scales make these systems challenging for theorists. For instance, the microscopic origin of the chiral order in the nematic phase of fd-viruses is still unresolved [32]. However, a recent study showed that in some cases the phase behaviour of fd-virus suspensions can be mapped onto that of hard rods [33], suggesting a dominant role of entropy in their self-assembly. Peculiar of these hard-rod-like suspensions is the formation of a columnar phase at high densities, whose stabilisation mechanism remains unclear. It is therefore interesting to investigate whether or not a columnar phase can be stabilised in a suspension of rod-like particles by entropy alone.

We term the columnar phase observed in rod-like particle systems as prolate columnar Col_+ to be distinguished from its oblate counterpart Col_- observed in systems of disk-like particles [16,35,36]. In both cases, the

orientation of the columns formed by the particles is parallel to the nematic director. However, in the case of the Col_- phase, the nematic director corresponds to the orientational order of the shortest particle axis, whereas for Col_+ the nematic director is related to the longest particle axis.

In 1987, a Col_+ phase was observed in pioneering simulation studies on hard parallel spherocylinders by Frenkel *et al.* [37]. However, a subsequent study by the Frenkel group [38] showed that this phase becomes mechanically unstable for sufficiently large system sizes. Similarly, the Col_+ phase was observed in small systems of freely rotating hard spherocylinders [39,40], but was argued to be thermodynamically unstable for larger systems [22,39]. In Section 3.1, we confirm that the Col_+ phase is indeed unstable for a system of freely rotating hard spherocylinders even at length-to-diameter ratios as extreme as $L/D = 100$. More intriguingly, perhaps, three independent simulation studies appeared in recent literature that reported the observation of a Col_+ phase in various systems of hard particles. In Ref. [41], a Col_+ phase was observed in the phase diagram of bent spherocylinders in a very narrow range of bending angles close to 180° , whereas Ref. [42] reported a Col_+ phase in systems of top-shaped rods, which consist of a hard spherocylinder with a larger hard sphere embedded in its centre. Finally, a stable Col_+ phase was reported in a large region of the phase diagram of hard cuboidal particles in Ref. [43].

Inspired by the experimental observation of the Col_+ phase in suspensions of fd-viruses, intrigued by the simulation results of Refs. [41–43], and with the knowledge of the finite-size effects reported by Veerman and Frenkel in Ref. [38], we investigate whether or not the Col_+ phase can be stabilised by entropy alone. This paper is organised as follows. The simulation methods are described in Section 2. We investigate the stability of the columnar phase in systems of (freely rotating) hard spherocylinders in Section 3.1, top-shaped rods in Section 3.2, cuboids in Section 3.3 and crooked rods in Section 3.4. Clearly, the systems investigated here do not represent an attempt to model suspensions of fd-viruses but they rather provide a useful playground for our search of an entropy-driven stabilisation mechanism for the Col_+ phase. Furthermore, these particle shapes can be directly linked to other experimental systems, as synthesis protocols exist to modulate the diameter of silica rods [44] or to bend them [45]. However, as it will be evident from our results, the Col_+ phase reported for these systems were due to simulations artefacts: the Col_+ phase becomes mechanically unstable when a sufficiently large system size is simulated. In Section 4, we conclude our study by speculating about other possible stabilisation

mechanisms for the Col_+ phase that might be relevant for fd-virus suspensions.

2. Simulation methods and order parameters

We perform standard Monte Carlo (MC) simulations in the NPT ensemble [46] of single-component systems of colloids with different shapes. The particles interact via a hard-core potential:

$$U(\mathbf{x}_i, \mathbf{x}_j) = \begin{cases} \infty, & \xi(\mathbf{x}_i, \mathbf{x}_j) < \sigma(\mathbf{x}_i, \mathbf{x}_j), \\ 0, & \xi(\mathbf{x}_i, \mathbf{x}_j) \geq \sigma(\mathbf{x}_i, \mathbf{x}_j), \end{cases} \quad (1)$$

where \mathbf{x} indicates the generalised coordinates (positions and orientations), $\xi(\mathbf{x}_i, \mathbf{x}_j)$ the centre-to-centre distance between particles i and j and $\sigma(\mathbf{x}_i, \mathbf{x}_j)$ the ‘thickness’ of the two hard bodies in that particular configuration. In the case of uniaxial particles, the particle orientation is described by a unit vector \mathbf{u} , whereas in the case of biaxial shapes either a 3×3 rotation matrix or a quaternion is employed, from which the orientation of the main axis \mathbf{u} is retrieved. For spherocylinders, top-shaped and crooked rods, the overlap algorithm is based on the explicit calculation of the minimum distance between two particles (using the efficient algorithm of Ref. [47]). For cuboids, we employ an intersection-detection algorithm based on the RAPID library [48]. To minimise the number of overlap checks in the case of strongly anisotropic particles, we divide the particle shape into smaller parts by fully covering the particles with a set of (overlapping) spheres with a diameter larger than the particle diameter. We then use these smaller parts to construct a cubic cell list as in the case of simple spheres [46,49]. These bounding spheres are used to identify the neighbours, whose overlaps are explicitly checked. By keeping track of the already checked particle pairs, this simple procedure speeds up substantially the simulations.

We employ a cuboidal simulation box with periodic boundary conditions to simulate N particles, typically arranged in n layers, at fixed (reduced) pressure $\beta P v_0$, where v_0 is the particle volume, $\beta = 1/k_B T$, k_B the Boltzmann constant, and T the temperature. One MC cycle consists of N attempts to either translate or rotate a randomly selected particle, and one attempt to either isotropically scale the system or scale just one (randomly selected) side of the simulation box. In the case of top-shaped and crooked rods, we also employ the ‘floppy-box’ method [50] to obtain the closest-packed configurations and the NPT -MC simulations are performed by using a variable box shape, for which also shear moves are performed to change the simulation box in addition to the scaling moves. We highlight that for anisotropic convex

particles, overlap checks must be performed both after compression and after an anisotropic expansion of the simulation box. For nonconvex particles, overlaps need to be checked also after isotropic expansions.

We determine the equation of state of the system, i.e. reduced pressure $\beta P v_0$ as a function of packing fraction $\eta = N v_0 / V$ with V being the volume of the simulation box, by averaging η over equilibrated configurations. In addition, we employ several order parameters to distinguish the different liquid crystal phases. We focus on the order associated with the main particle axis, also in the case of biaxial particles. In particular, we calculate the (scalar) nematic order parameter $S_{\mathbf{u}}$ by diagonalising the tensor

$$\mathcal{Q}_{\alpha\beta}^{\mathbf{u}} = \frac{1}{N} \sum_{i=1}^N \left[\frac{3}{2} \mathbf{u}_{i\alpha} \mathbf{u}_{i\beta} - \frac{\delta_{\alpha\beta}}{2} \right], \quad (2)$$

where $\alpha, \beta \in \{x, y, z\}$, $i = 1, \dots, N$, and $\delta_{\alpha\beta}$ is the Kronecker delta. The largest eigenvalue of \mathcal{Q} is $S_{\mathbf{u}}$ and the corresponding eigenvector is the nematic director $\mathbf{n}_{\mathbf{u}}$. In order to check the mechanical stability of the Col_+ phase with respect to the smectic and crystal phase, it is crucial to detect the formation of smectic layers. To this end, we employ the smectic order parameter $\tau_{\mathbf{u}}$ to quantify the degree of layering

$$\tau_{\mathbf{u}} = \max_l \left| \sum_{j=1}^N \exp \left(\frac{2\pi}{l} \mathbf{ir}_j \cdot \hat{\mathbf{n}}_{\mathbf{u}} \right) \right|, \quad (3)$$

where $l \in \mathcal{R}$ is a real number and \mathbf{r}_j denotes the position of particle j . A large $\tau_{\mathbf{u}}$ indicates layering in a direction parallel to the nematic director $\mathbf{n}_{\mathbf{u}}$. The value of l that maximises $\tau_{\mathbf{u}}$ corresponds to the smectic layer spacing d , which is the characteristic length scale of the one-dimensional positional order in that direction. For the biaxial particles in Section 3.3, Equations (2) and (3) are straightforwardly modified to also quantify the order associated to the short particle axis (see also Ref. [27]). When the layering does not occur along $\mathbf{n}_{\mathbf{u}}$, as in Section 3.2, we consider a very large number of directions \mathbf{n}_i , equispaced on half of the unit sphere, and calculate τ_i as in Equation (3) for each of these directions. Analogously, a large τ_i indicates positional order along direction \mathbf{n}_i with a characteristic spacing d_i . In this way, the direction of the most pronounced layering can be identified. More than one layering direction is found in systems that exhibit 2 or 3 degrees of positional order (e.g. columnar or crystal phases). In addition, we also calculate the tilt angle θ of the layering direction \mathbf{n}_i with the nematic director $\mathbf{n}_{\mathbf{u}}$. Finally, we confirm the identification of the different liquid crystal phases by calculating the diffraction patterns as obtained by projecting the

particle positions on a predefined plane and calculating the Fourier transform of a two-dimensional histogram of the projected positions.

3. The quest of a prolate columnar phase

3.1. Hard spherocylinders: the exemplary case of colloidal liquid crystals

We first study a system of hard spherocylinders, consisting of a cylindrical part of length L and diameter D capped by two hemispheres with the same diameter at both ends (see inset of Figure 1). This particle system was employed by Frenkel *et al.* to demonstrate, for the first time in computer simulations, that a smectic phase can be stabilised by entropy alone [15]. Since then, a significant number of theoretical and simulation studies have been carried out investigating the structure, thermodynamics and dynamics of hard spherocylinders, and the phase diagram of this system is now, largely due to a detailed study based on free-energy calculations by Bolhuis and Frenkel [39], well established [22,39,40]. In Figure 1, we present the phase diagram of Ref. [39] in the packing fraction η -aspect ratio L/D representation. We note that we converted the reduced density scale of the original phase diagram to packing fractions here to facilitate comparisons with experiments and other simulation studies. Apart from the plastic crystal (P) occurring at low aspect ratio, the thermodynamically stable positionally ordered phases are the smectic (Sm) and the crystal (X) phase, consisting of particles arranged in layers. Based on the in-plane order in each layer and the correlations between the layers, a further classification can be made: spherocylinders form a stable Sm -A phase when the particles display a liquid-like structure within each plane, and a stable crystal X phase when the particles

show long-range hexagonal positional order with either AAA or ABC stacking of the hexagonal layers. In the AAA- X phase, the hexagonal layers are exactly on top of each other, whereas in the ABC- X phase the layers are shifted with respect to each other, equivalently to a face-centred-cubic crystal that is stretched in the direction perpendicular to the hexagonal planes to accommodate the spherocylinders. The relative thermodynamic stability between the two types of stackings depends both on the aspect ratio L/D and the packing fraction η . The ABC- X phase is stable at all η for $L/D < 7$. For longer rods, the AAA- X phase is stable at low η and transforms into the ABC- X phase at sufficiently high η , see Ref. [39]. In the case the hexagonal positional order persists, but the layers are uncorrelated, the phase is identified as a smectic-B phase. The latter has been observed in experiments on suspensions of silica rods [12].

In this work, we aim to study whether or not a Col_+ phase can be stabilised in a system of hard rods. As mentioned in Section 1, the Col_+ phase has first been observed in small systems of parallel hard spherocylinders [37], but was later on proven to be mechanically unstable in larger systems [38]. There is no reason to expect that spherocylinders with rotational degrees of freedom would stabilise a Col_+ phase, which is also conjectured in Ref. [22] and is consistent with the phase diagram of Ref. [39]. In order to verify this for once and for all, we perform simulations on freely rotating spherocylinders with an aspect ratio of $L/D = 5, 10$ and 100 . We arrange the particles in hexagonal layers with either AAA or ABC stacking, and use either $n = 3$ or $n = 6$ layers. The number of particles is $N = 300$ in the case of $n = 3$, and we double the number of particles in the case of $n = 6$. We use these four structures as initial configurations for the MC simulations in the NPT ensemble. We fix the pressure $\beta P v_0$ and number of particles N , and monitor

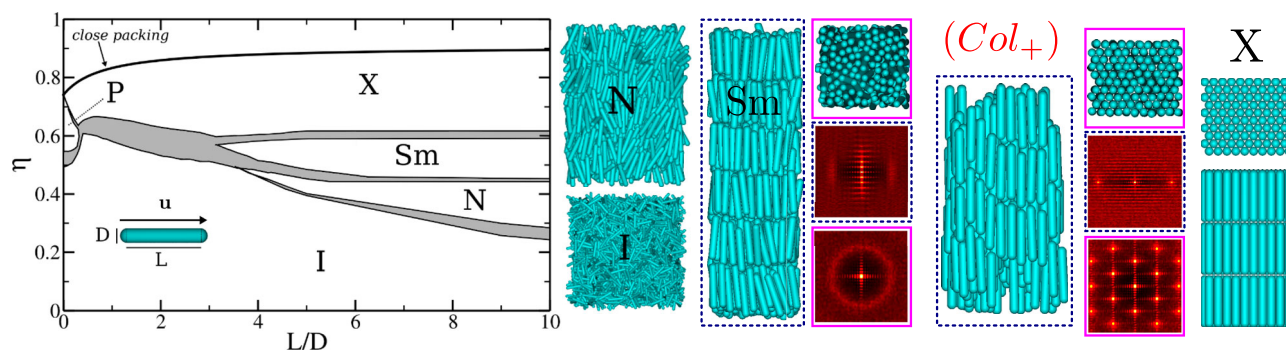


Figure 1. Phase diagram of hard spherocylinders in the packing fraction η -aspect ratio L/D representation, data adapted from Bolhuis and Frenkel [39]. The different stable phases indicated in the phase diagram are: isotropic (I), plastic crystal (P), nematic (N), smectic (Sm) and crystal (X) phase. Representative snapshots of isotropic, nematic, smectic (metastable), prolate columnar (Col_+) phase and crystal phase (X) with the AAA stacking are also shown. For the last three phases, both top and side views are shown. For Sm and Col_+ phases, the diffraction patterns obtained by projecting the particle positions onto the respective plane (top and side view) are also shown.

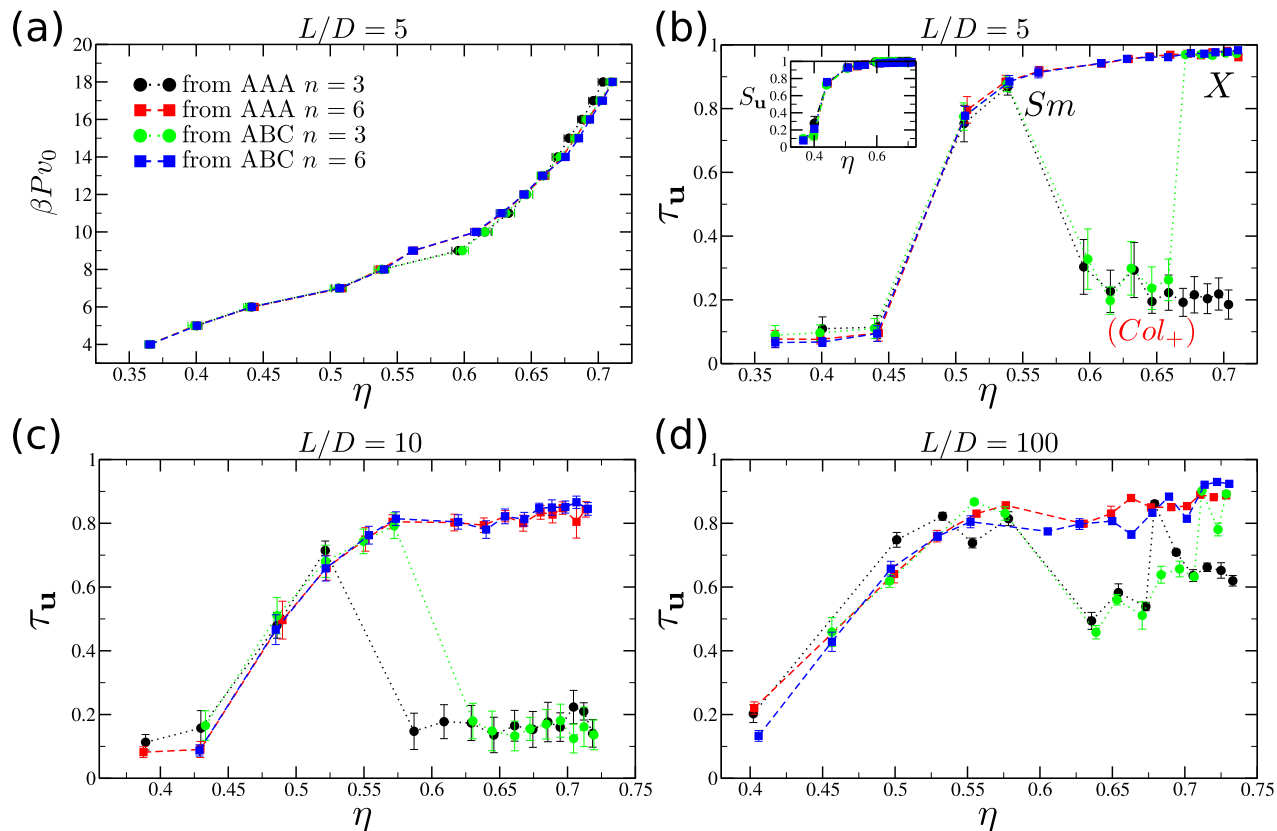


Figure 2. (a) Equation of state (reduced pressure $\beta P v_0$ as a function of packing fraction η) for hard spherocylinders with aspect ratio $L/D = 5$ obtained via NPT -MC simulations starting from different initial configurations (AAA or ABC stacking) with a different number of particle layers n , as indicated in the legend. (b) Smectic order parameter τ_u as a function of η for spherocylinders with $L/D = 5$ starting from different initial configurations. The keys of the legend are the same as in (a). For $n = 3$ a metastable Col_+ appears. Inset: nematic order parameter S_u as a function of packing fraction η . (c,d) The same as (b) for aspect ratio $L/D = 10$ and $L/D = 100$.

the structural properties after equilibration using the nematic and smectic order parameters. In Figure 2(a), we plot the equation of state of hard spherocylinders with $L/D = 5$. We observe a difference in the equation of state for a system of $n = 3$ and $n = 6$ layers, indicating a size dependence of the phase behaviour. The nematic order parameter S_u (inset) and the smectic order parameter τ_u are plotted in Figure 2(b). The former is basically insensitive to the system size. The latter, however, shows a large increase at the $N-Sm$ transition, but drops drastically for the system of $n = 3$ layers, signalling the absence of particle layering and the formation of a Col_+ phase, as can also be appreciated from the snapshots in Figure 1. The range of packing fractions η , for which we observe the Col_+ phase, is smaller when we use a system with an ABC stacking. This might be related to the fact that the AAA stacking transforms more easily into a Col_+ phase since the particles are already arranged in columns, and to the fact that the ABC crystal is stable for $L/D = 5$. If we employ a system of $n = 6$ layers, the drop in τ_u that signifies the transition to the Col_+ phase is absent,

irrespective of the initial stacking. Similar simulations are performed for larger aspect ratios. In Figure 2(c), we present the smectic order parameter τ_u for $L/D = 10$, and in Figure 2(d) for $L/D = 100$. We remark here that $L/D = 100$ corresponds to the range of aspect ratios of fd-viruses. For $L/D = 10$, we again observe a drastic decrease of τ_u for systems with $n = 3$ irrespective of the stacking, but we find no drop in the case of a larger system with $n = 6$ layers. This drop occurs at higher η if the initial configuration is ABC-stacked, consistent with the fact that the formation of columns in this configuration is hindered by the type of stacking and the layering can survive for a larger range of η . For $L/D = 100$, the decrease in τ_u , although still present for $n = 3$, appears smaller, suggesting that the finite-size effects might be less severe in this case. We conclude that in the case of hard spherocylinders the Col_+ phase is mechanically unstable irrespective of the aspect ratio of the particles. In the next sections, we modify the particle models to search for possible shape features which may favour the stabilisation of a Col_+ phase.

3.2. Modulating the diameter: top-shaped rods

We modify the particle shape by considering top-shaped rods [42], a minimal model for mimicking rods with a larger diameter in the middle. The particles consist of a hard spherocylinder with an aspect ratio L/D and a hard sphere with a sphere-to-rod-diameter ratio σ/D embedded in its centre. Since the top-shaped rods are uniaxial, the orientation is fully described by the unit vector \mathbf{u} , see Figure 3(a). In Ref. [42], a density functional theory was employed to determine the liquid crystal behaviour of parallel top-shaped rods using various approximations. Irrespective of the aspect ratio, a region of stability of the Col_+ was predicted for intermediate values of σ/D at sufficiently high packing fractions η . For small σ/D the phase behaviour of spherocylinders was recovered, while for large σ/D a tilted smectic-C was predicted. Additionally, simulation results obtained by compressing small systems, $N = 256$, of parallel top-shaped rods with $L/D = 9$ were presented in Ref. [42] for very small $\sigma/D \leq 1.06$ and for $\sigma/D = 1.80, 1.85, 1.90$. In the first case, a drop in

the smectic order parameter τ_u , signifying the formation of a Col_+ phase, was observed upon increasing η , reminiscent of the spherocylinder behaviour. For large σ/D , the jump in the order parameter τ_i at $\eta \simeq 0.45$ (in our notation), corresponding to a layering along a direction $\mathbf{n}_i \neq \mathbf{n}_u$ (see Section 2), signalled the onset of a tilted phase.

In this section, we carry out simulations on systems of freely rotating top-shaped rods with the same aspect ratio as in Ref. [42], i.e. $L/D = 9$. We first focus on the case of $\sigma/D = 1.1$, for which we expect a behaviour similar to that of spherocylinders. We observe that a Col_+ phase is formed in systems with $n=4$ layers but this phase disappears if the number of layers n is doubled, as shown schematically in Figure 3(b). To be more specific, we initiate our simulations from configurations consisting of $n=4$ hexagonal layers with an AAA stacking and arranged along the z -direction in a cuboidal simulation box. We subsequently perform standard NPT-MC simulations at different pressures until the system

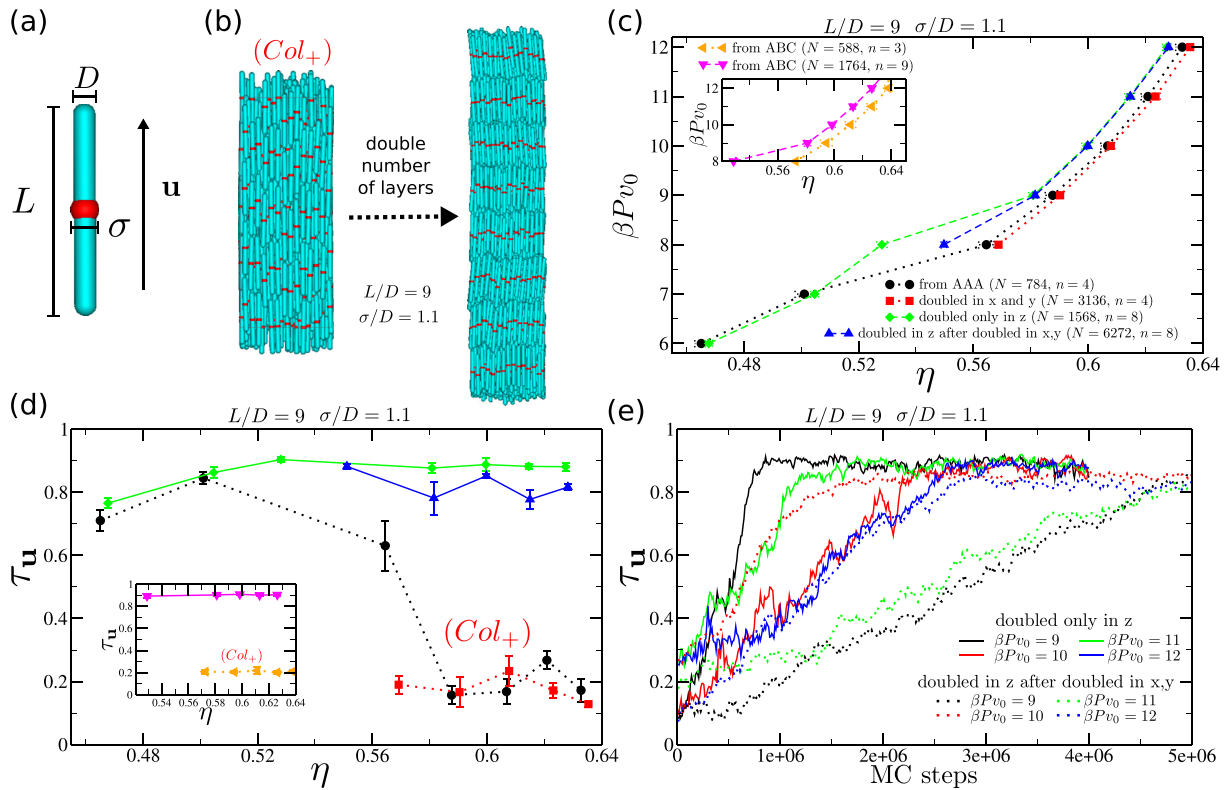


Figure 3. (a) Model of a top-shaped rod. (b) Snapshots representing how a Col_+ phase transforms into a layered smectic phase when the number of layers is doubled for top-shaped rods with $L/D = 9$ and $\sigma/D = 1.1$. (c) Equation of state of top-shaped rods with $L/D = 9$ and $\sigma/D = 1.1$ obtained via NPT-MC simulations starting from different initial configurations with different numbers of layers n as indicated in the legend (see main text). Inset: equation of state obtained from initial configurations with ABC stacking. (d) Smectic order parameter τ_u as a function of η obtained via NPT-MC simulations for different initial configurations. The keys are the same as in (c). Inset: starting from ABC stacking. The appearance of the metastable Col_+ is indicated. (e) Evolution of the smectic order parameter τ_u in NPT-MC simulations at different pressure $\beta P v_0$ when the number of layers of the (previously equilibrated) initial configuration, that is a Col_+ phase, is doubled (from $n = 4$ to $n = 8$). All the systems equilibrate to a layered configuration in a number of steps that has no clear dependence on the pressure and the system size in the x - and y -directions (perpendicular to the layering).

forms a Col_+ phase and is well equilibrated. From the final configurations (at each pressure), we generate a new configuration by either (i) duplicating the system in the direction of the layers (z -direction), i.e. doubling n , or (ii) duplicating the system in the x - and y -directions orthogonal to the layering, thereby keeping n fixed. New runs of NPT -MC simulations are then performed starting from the new configurations until equilibration. The final configurations of type (ii) are then replicated along the z -direction thereby doubling n , and again equilibrated using NPT -MC simulations. Using this simulation procedure, we can not only verify if the Col_+ phase becomes mechanically unstable when the number of layers n is doubled, but can also check if doubling the system size perpendicularly to the layering direction affects the stability of the Col_+ phase. In Figure 3(c), we report the equation of state for all the simulations carried out and we observe a clear finite-size effect. Figure 3(d) clearly shows that the Col_+ phase is only observed for a system of $n = 4$ layers, as evident from the drop of τ_u at $\eta \simeq 0.57$. In Figure 3(e), we report the evolution of τ_u as a function of MC steps for the runs in which the initial Col_+ configuration has been doubled in the z -direction. Figure 3(e) shows clearly that initially the system with a low $\tau_u \simeq 0.2$ corresponds to the Col_+ phase, but τ_u increases steadily with MC steps as the system transforms into a smectic phase. We find no clear dependence on the pressure and on the system size in the x - and y -directions (perpendicular to the layering). We conclude that the number of layers n is the key parameter in the formation of the Col_+ phase, and that other factors only play a marginal role. Finally, the insets of Figure 3(c,d) show the simulation results starting from an ABC stacking with either $n = 3$

or $n = 9$ layers, corroborating the conclusion that Col_+ is obtained only for small n , irrespective of the stacking configuration.

We now consider top-shaped rods with a larger sphere diameter $\sigma/D = 1.3, 1.5, 1.7, 1.9$, and perform similar sets of simulation runs. The equations of state obtained starting from an AAA stacking with $n = 4$ layers and the smectic order parameter τ_u as a function of η are shown in Figure 4(a). We immediately note that in the case of large σ/D no discontinuity is observed in density (or only at extremely large pressures), suggesting the absence of any phase transformation. This might be due to the fact that the AAA-stacked configuration is not the close-packed structure and imposing a high pressure might lead to jamming. In Figure 4(b–e), we show typical configurations of the larger systems at high pressure. Visual inspection of these configurations, together with the trends of τ_u (inset of Figure 4(a)), suggests that the Col_+ phase is stable for $\sigma/D = 1.3$, the smectic phase is observed for $\sigma/D = 1.5$, distorted/tilted order is observed for $\sigma/D = 1.7$, and no positionally ordered phase is obtained for $\sigma/D = 1.9$. In order to check if these simulation results were affected by the cuboidal simulation box that might be incommensurate with the equilibrium structure of these rods, we resort to the floppy-box MC method [50] to determine the closest-packed structures with two particles in the unit cell as shown in Figure 5. These structures consist of intercalated hexagonal layers of particles tilted with respect to the nematic director. We use these crystal structures as starting configurations in our NPT -MC simulations with a variable box shape. In Figure 6(a), we show the resulting equations of state. We observe a strong first-order

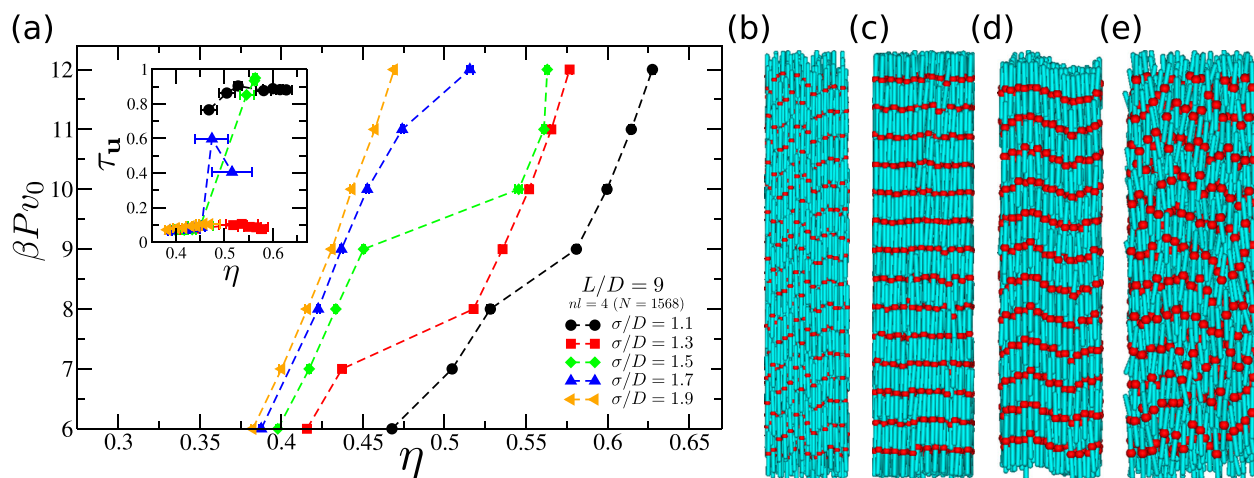


Figure 4. (a) Equations of state for top-shaped rods with $L/D = 9$ and different sphere-to-rod diameter ratios σ/D obtained via NPT -MC simulations using a cuboidal simulation box. The inset shows the smectic order parameter τ_u as a function of packing fraction η . (b–e) Snapshots of the final configurations obtained for larger systems using a cuboidal simulation box at $\beta P v_0 = 12$ for (b) $\sigma/D = 1.3$, (c) $\sigma/D = 1.5$, (d) $\sigma/D = 1.7$ and (e) $\sigma/D = 1.9$.

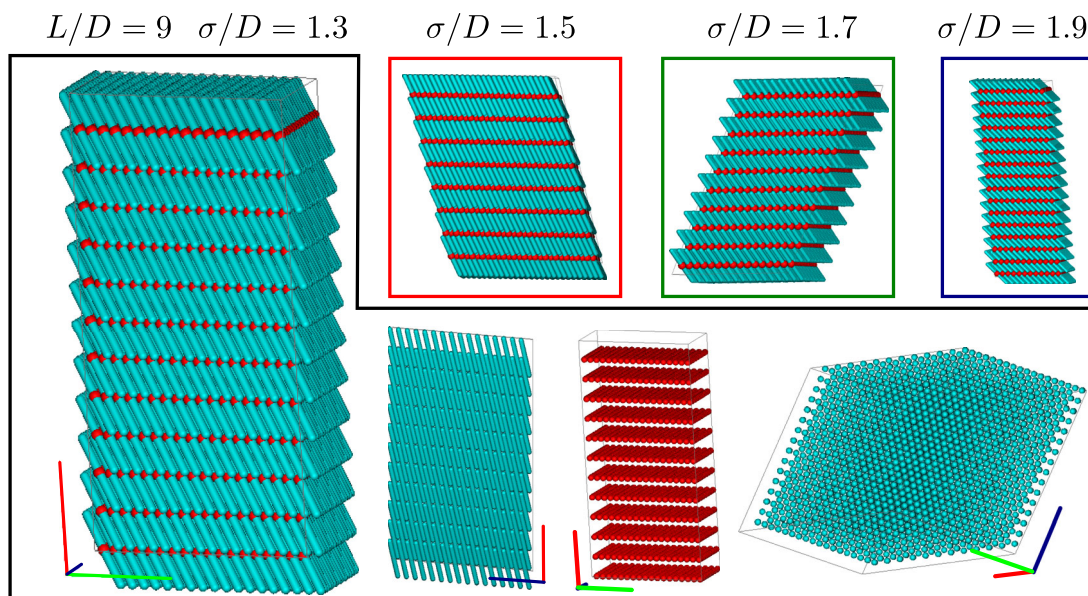


Figure 5. Snapshots of the close-packed configurations for top-shaped rods obtained via the floppy-box MC method with two particles in the unit cell. For $\sigma/D = 1.3$ different orientations of the configuration with only the spherocylinder component or only the central sphere of the top-shaped rods are shown.

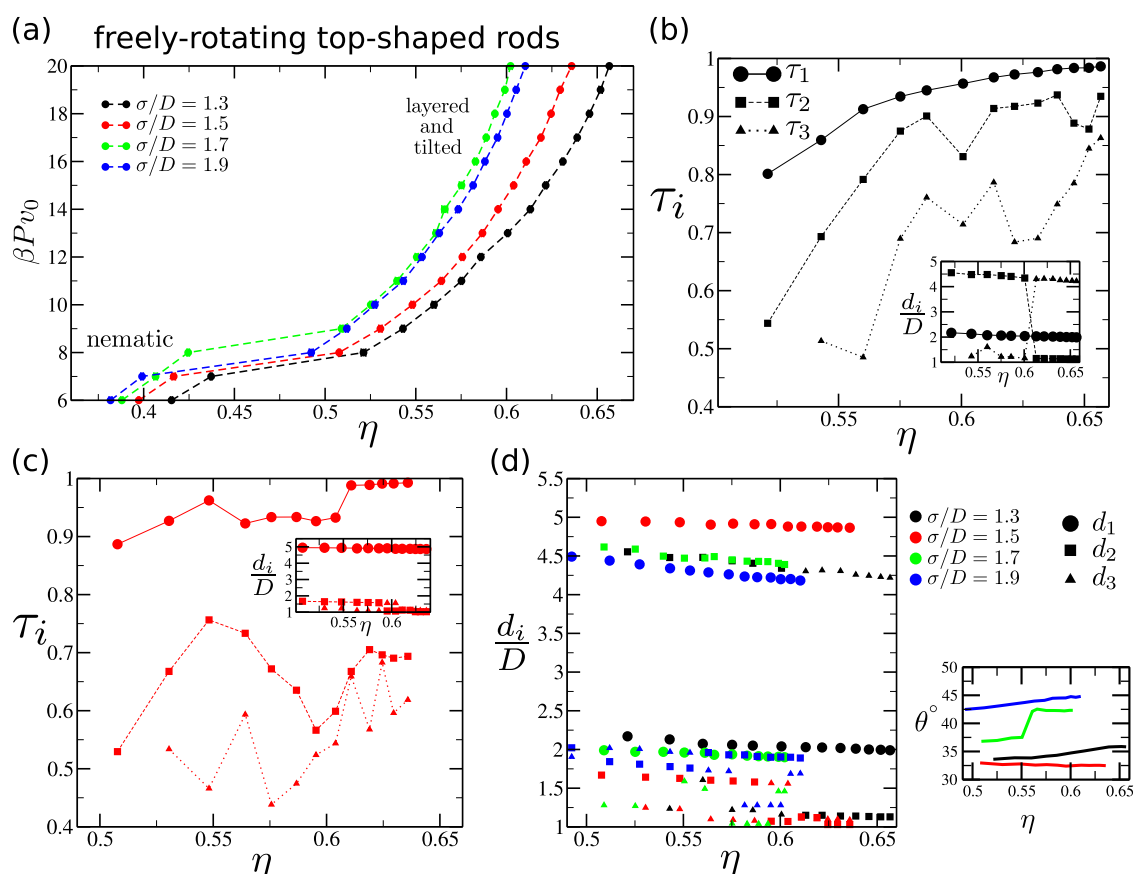


Figure 6. (a) Equation of state for freely rotating top-shaped rods obtained via *NPT*-MC simulations using a variable box shape and starting from the close-packed configurations of Figure 5. (b) The three largest layering order parameters τ_i and the associated spacing d_i (in units of D , inset) as a function of packing fraction η for top-shaped rods with $\sigma/D = 1.3$. (c) Same as in (b) for $\sigma/D = 1.5$. (d) The layer spacing d_i associated to the three largest layering order parameters as a function of η for all the four values of σ/D (colours in the online version are indicating σ/D whereas symbols are indicating ranking). The small graph shows the tilt angle θ between the nematic director and the layering direction with the largest d_i as a function of η .

phase transition at a pressure $\beta P v_0 \simeq 8.0$ with coexisting packing fractions of $\eta \simeq 0.45$ and $\eta \simeq 0.50$. At low pressures the system forms a nematic phase. To characterise the structure at high pressures, we identify the directions of the most pronounced layering as the (three) directions \mathbf{n}_i associated to the largest value $\tau_i > 0.4$ (see also Section 2). We report the values of τ_i as well as the layer spacing d_i along the respective direction \mathbf{n}_i in Figure 6(b–d). The symbols in the figures are coloured (in the online version) according to σ/D and their shape represents the values of the associated τ_i (circle, square, triangle for the largest, second, third τ_i , respectively). Focusing on Figure 6(b), we observe that the system displays long-range positional order in three different directions in the entire range of η (except for the first value of η). The corresponding spacings d_i are plotted in the inset and summarised in Figure 6(d), from which it is clear that in all cases the high-pressure states consist of intercalated layers with a significant spacing $d_i \sim L/2D$. Furthermore, we find long-range positional order also in two other directions with typical spacings $d_i \leq 2.2D$. We therefore conclude that the structure is crystalline. Exceptions are the states corresponding to the lowest value of η both in Figure 6(b,c), where positional order ($\tau_i > 0.4$) is only detected in two directions with one of the two directions corresponding to the intercalated layering of these rods. One explanation might be that the columnar phase is different from Col_+ , or that the positional order is too weak to be detected as these states are close to the melting transition to the nematic phase. Finally, in Figure 6(e) we also plot the tilt angle θ between the direction of the layers with spacing $d_i \sim L/2D$ and the nematic director. The layers become more tilted upon increasing packing fraction η . In addition, we note a significant jump in the tilt angle for $\sigma/D = 1.7$ at $\eta \simeq 0.55$ indicating a structural reorganisation of the layers, which is also accompanied with a small discontinuity in the equation of state. We remark that in Ref. [42] a larger tilt angle and a much smaller spacing were reported. This discrepancy is only noticeable, as the tilt angle here is defined as the one associated to the largest layer spacing d_i and not to the largest τ_i . If we use the same definitions as in Ref. [42], the results are in reasonable agreement. However, we stress once more that in Ref. [42] a system of parallel top-shaped rods was considered, for which no rotational entropy is present. Since for top-shaped rods the rotational entropy in a smectic phase should be larger than it is in a Col_+ phase, and its difference should increase by increasing σ/D , the stability of a Col_+ might be more likely if the particles cannot freely rotate. For this reason, we also perform NPT -MC simulations for large systems of parallel top-shaped rods with $L/D = 9$ and $\sigma/D = 1.3$ ($N = 3072$), $\sigma/D = 1.5$ ($N = 3840$), $\sigma/D =$

1.7 ($N = 2560$) and $\sigma/D = 1.9$ ($N = 2304$). In particular, we expand close-packed configurations obtained via the floppy-box method (imposing that the two particles in the unit cell must have the same orientation) in the NPT ensemble by setting the pressure $\beta P v_0$ and run for 10^7 MC steps. The obtained equations of state together with the layering analysis are reported in Figure 7. We observe that the positional order sets in at similar packing fractions and lower pressures than for freely rotating rods, as expected. Also for parallel top-shaped rods, the majority of the state points simulated correspond to crystal structures, i.e. there are three large τ_i . In all cases when positional order is observed, there is a layer spacing $L/3D < d_i < L/2D$ indicating that the intercalated layered structure is strongly tilted (see, for example, Figure 7(c)). As before, for some cases close to the melting to the nematic phase (see, for example, Figure 7(f)), positional order is detected only in two directions, one being the layering direction conventionally expected in a smectic phase of prolate particles.

To summarise, our simulations lend support that the Col_+ phase is absent in large systems of (freely rotating or parallel) hard top-shaped rods with $L/D = 9$ as the layering remains intact for the entire stability range of positionally ordered states, when a floppy simulation box is used.

3.3. Being biaxial: cuboidal particles

We now investigate the effect of biaxiality on the stability of the Col_+ phase. To this end, we consider rod-like particles with a cuboidal shape. We define L , M and S as the long, medium and short particle length, as shown in Figure 8(a). We expect that the particles form a columnar phase with a rectangular in-plane order rather than a hexagonal order, which might affect the stability of the Col_+ phase with respect to the smectic or crystal phase.

The phase diagram of cuboids with reduced length $L^* = L/S = 9$ and 12, and various $M/S \leq L^*$ have been studied in Ref. [43]. Surprisingly, a Col_+ phase was reported for shapes close to $M = S$ in a quite large packing fraction range, abruptly invading the region where a crystal phase is to be expected. The number of particles in these simulations was quite large, ranging from $N = 1100$ to $N = 3500$, but the Col_+ was observed in systems with only $n = 4$ layers. Interestingly, for less anisotropic cuboids, $L^* = 9$, the range of values of M/S for which Col_+ was found is smaller than for more anisotropic particles, i.e. $L^* = 12$.

In this work, we consider cuboidal rods with $M = S$ and (reduced) lengths ranging from $L^* = 5$ to $L^* = 12$. Cuboids with $M = S$ and $L^* \leq 5$ were already studied in Ref. [51]. In this study, a Col_+ phase was also observed

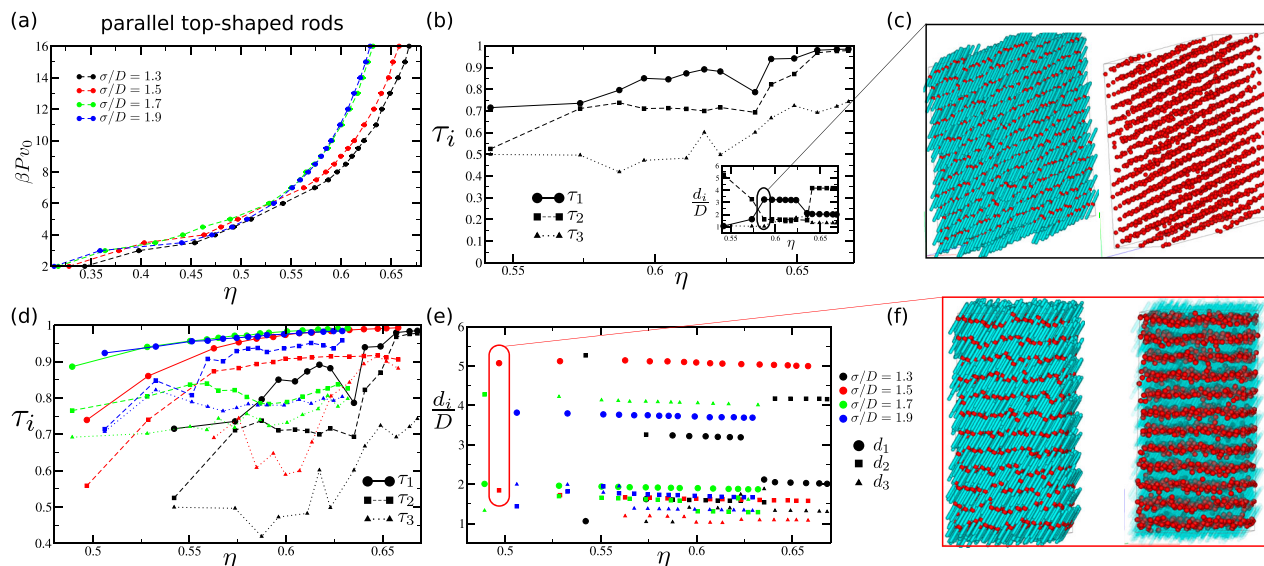


Figure 7. (a) Equation of state for parallel top-shaped rods obtained via *NPT*-MC simulations using a variable box shape and starting from close-packed configurations. (b) The three largest layering order parameters τ_i and the associated spacing d_i (inset) as a function of η for parallel top-shaped rods with $\sigma/D = 1.3$. (c) Representative snapshots for $\sigma/D = 1.3$ and $\beta P v_0 = 7$. The same configuration is shown with or without the spherocylindrical part of the rods. (d) The three largest layering order parameters τ_i and (e) the associated layer spacing d_i as a function of η for all the four values of σ/D (colours in the online version are indicating σ/D whereas symbols are indicating ranking). (f) Representative snapshots for $\sigma/D = 1.5$ and $\beta P v_0 = 4$. The same configuration is shown with a solid or transparent spherocylindrical part of the rods.

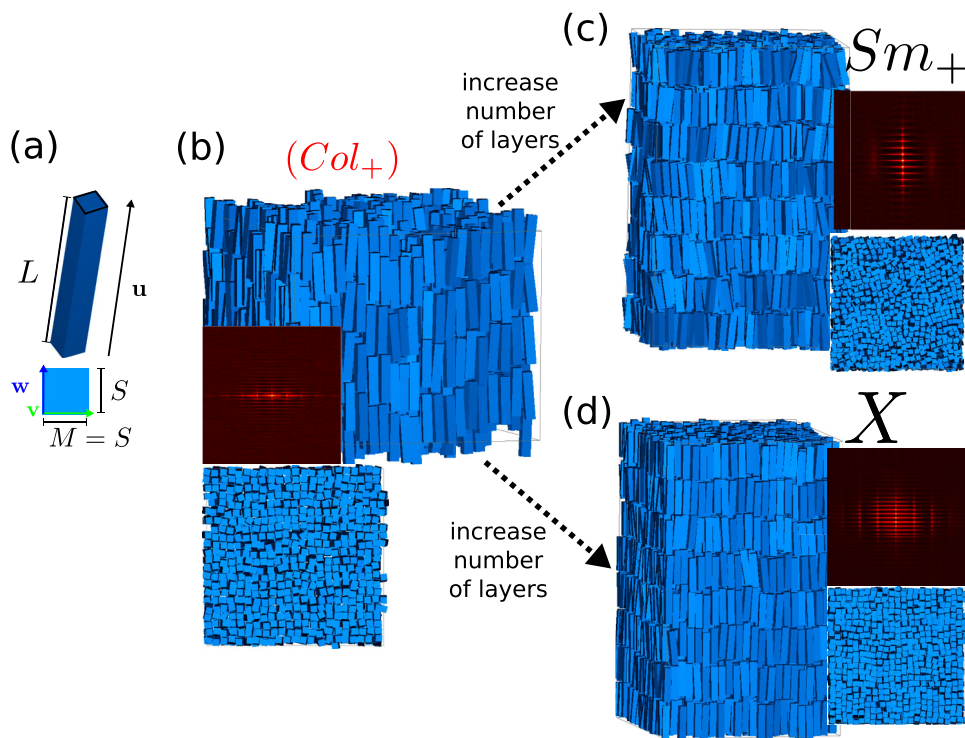


Figure 8. (a) Model of hard cuboidal rods. The particle shape is defined via the lengths of the three main particle axis (L, M, S) and its orientation is described by using the vectors $\mathbf{u}, \mathbf{v}, \mathbf{w}$. In this study, we consider only particles with $M = S$. (b) Representative snapshots (top and side view) of a prolate columnar phase (Col_+) obtained via *NPT*-MC simulations of $N = 1936$ cuboids (corresponding to a number of layers $n = 4$) with $L^* = 5$ ($\beta P v_0 = 8.0$). The inset shows the corresponding diffraction pattern, obtained by projecting the particle positions onto the plane containing the main two nematic directors (corresponding to the side view snapshot). By increasing the number of layers n (and therefore N) the Col_+ phase is unstable with respect to either (c) a (prolate) smectic phase (Sm_+) ($L^* = 5$, $\beta P v_0 = 7.0$) or (d) a crystal phase (X) ($L^* = 5$, $\beta P v_0 = 10.0$), depending on the packing fraction (or equivalently the imposed pressure). Both side and top view and the diffraction pattern associated to the side view are shown.

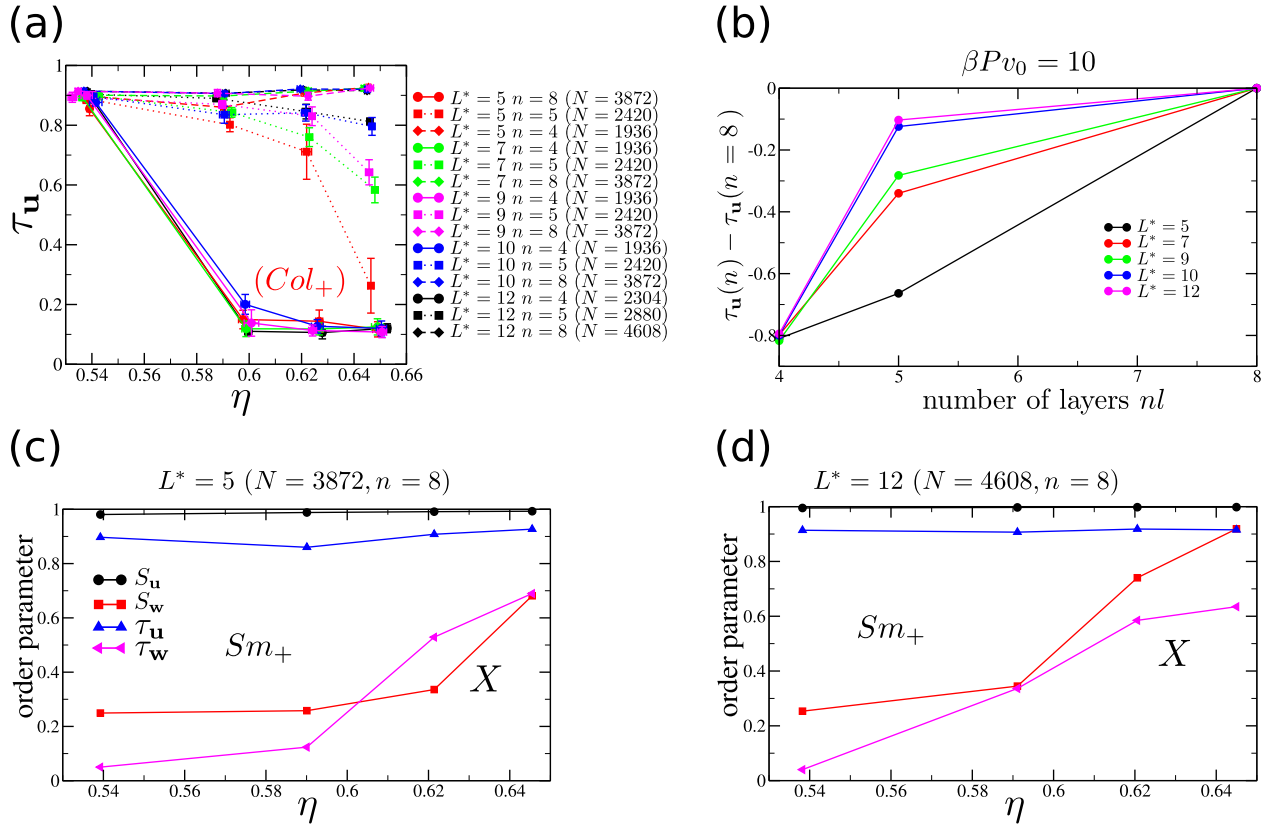


Figure 9. (a) Smectic order parameter τ_u as a function of packing fraction η for cuboidal rods with different aspect ratios $L^* = L/S$. The system sizes studied are indicated in the legend using the number of layers n in the initial configurations (and the corresponding total number of particles N). At $\eta \simeq 0.54$ all the systems studied exhibit a Sm_+ phase. For small system size, upon increasing η the smectic order decreases more or less drastically depending on n . (b) Difference in the smectic order parameter τ_u as obtained from NPT-MC simulations at high pressure ($\beta P v_0 = 10$) of systems with n layers with respect to a larger system ($n = 8$) for different aspect ratios L^* . The size effects are more pronounced for small L^* . (c,d) (Equilibrium) phase transition between the smectic phase Sm_+ and the crystal phase X for large systems of hard cuboids with aspect ratio $L^* = 5$ and $L^* = 12$, monitored by the nematic and smectic order parameters as indicated in the legend.

instead of an X phase in the case of small system sizes. However, the authors mentioned that particular attention should be paid at high packing fractions because of finite-size effects, which is consistent with observations made in a previous simulation study [52]. Here, we investigate whether or not the Col_+ phase becomes stable upon increasing the aspect ratio L^* of the cuboids.

We perform NPT-MC simulations on systems of cuboidal rods using different numbers of particle layers $n = 4, 5$ and 8 . We observe a Col_+ phase for $n = 4$ as shown in Figure 8(b), whereas in the case of $n = 8$, we find either a (prolate) smectic phase Sm_+ , see Figure 8(c), or a crystal phase X as shown in Figure 8(d), depending on the pressure. To quantify the finite-size effects, we plot in Figure 9(a) the smectic order parameter τ_u as a function of η for different L^* and n . At $\eta \simeq 0.54$ all systems show a Sm_+ phase. For $n = 4$, the order parameter τ_u drops abruptly upon increasing η , corresponding to the formation of the Col_+ phase. In the case of $n = 5$, the decrease is more gradual and shifted to larger η depending on L^* .

We find that τ_u never decreases below 0.9 for systems with $n = 8$ layers. In Figure 9(b), we report the difference in τ_u at pressure $\beta P v_0 = 10$ between systems with $n = 4, 5$ and with $n = 8$. Assuming that the latter are the equilibrium values of the smectic order parameter τ_u , we find that the finite-size effects are less pronounced upon increasing the aspect ratio of the rods, i.e. τ_u is closer to the equilibrium values for larger L^* . Finally, by looking at the order parameters associated to the short particle axis w as shown in Figure 9(c,d) for $L^* = 5$ and $L^* = 12$, we (roughly) identify the packing fraction intervals corresponding to the equilibrium Sm and X phases.

In conclusion, also cuboids exhibit a metastable Col_+ phase due to finite-size effects, irrespective of the anisotropy of the rods.

3.4. Bending the colloids: crooked rods

Finally, we consider crooked rods composed of two hard spherocylinders of aspect ratio L/D , sharing one of the

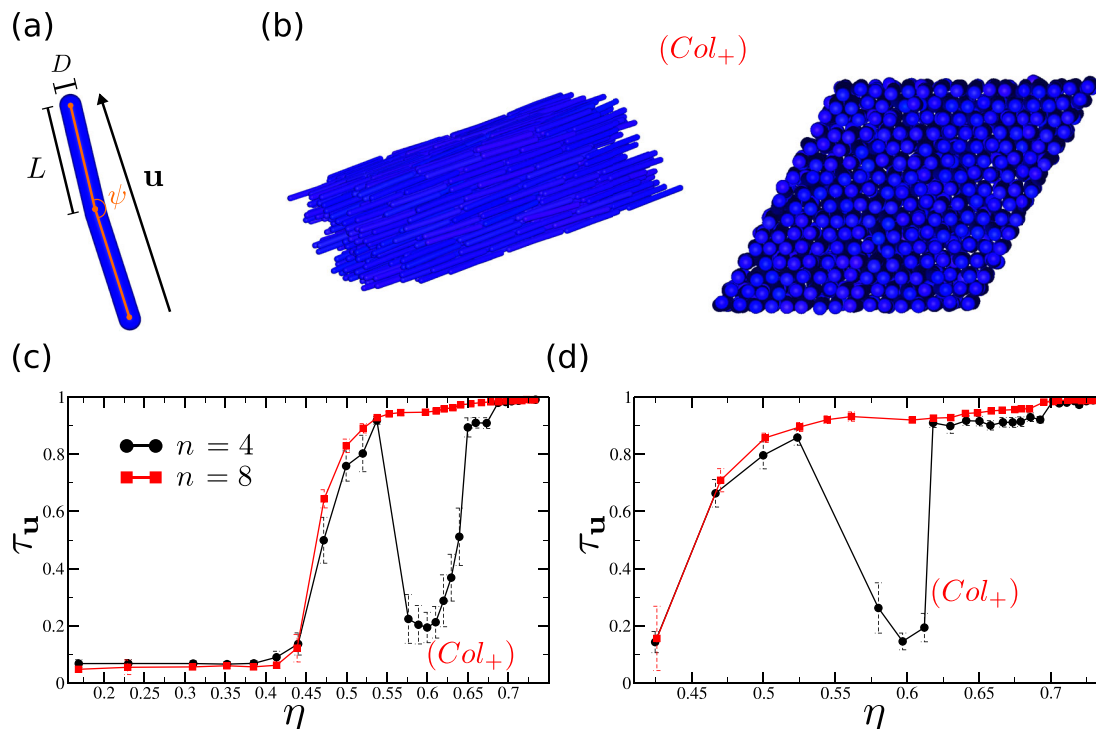


Figure 10. (a) Model of a hard crooked rod with bending angle $\psi = 175^\circ$ and $L/D = 5$. (b) Snapshots of the metastable prolate columnar Col_+ phase in two different orientations of the simulation box obtained for $n = 4$ layers of particles. (c) Smectic order parameter τ_u as a function of packing fraction η for crooked rods with $\psi = 175^\circ$ obtained by NPT-MC simulations with a variable box shape and with an initial configuration of $n = 4$ or $n = 8$ particle layers. (d) Same as in (c) for bending angle $\psi = 178^\circ$.

spherical end caps and merged together with a bending angle ψ , see Figure 10(a). Crooked rods are biaxial and polar, and these two properties can be transmitted to the macroscopic scale giving rise to an interesting variety of liquid crystal phases such as twist-bend and splay-bend nematic phases. The phase behaviour of hard crooked rods with $L/D = 5$ and bending angle $\psi \in [90^\circ, 180^\circ]$ was studied in Ref. [41] using simulations of $N = 400$ particles arranged in $n = 4$ layers. A Col_+ phase was reported close to the spherocylinder limit ($\psi \rightarrow 180^\circ$), even though the authors had some doubts about its thermodynamic stability. In this section, we study crooked rods with $L/D = 5$ and $\psi = 175^\circ$ and $\psi = 178^\circ$. We perform NPT-MC simulations with a variable box shape starting from an anti-polar crystal phase as obtained from the floppy-box MC method [50] with two particles in the unit cell. The initial configuration consists of either $N = 1024$ particles arranged in $n = 4$ layers or $N = 2048$ arranged in $n = 8$ layers. As before, we quantify the layering along the main nematic director via τ_u . In Figure 10(c,d), we plot τ_u as a function of η for $\psi = 175^\circ$ and $\psi = 178^\circ$, respectively. In both cases, there is an interval of η in which τ_u is small for $n = 4$ but large for $n = 8$, corresponding to the formation of a Col_+ phase for only small system sizes as depicted in Figure 10(b). The range of the Col_+ is larger for $\psi = 175^\circ$, when the

aspect ratio of the rods, defined by the end-to-end distance divided by the particle width, is smaller. This observation provides again support that the finite-size effects are stronger for less anisotropic particles. For crooked rods, the metastable Col_+ lies entirely inside the region in which an Sm phase is expected, i.e. the observed phase sequence in small systems is $Sm - (Col_+) - Sm - X$ upon increasing η . Moreover, the packing fraction range in which we observe Col_+ is smaller than what was found in Ref. [41]. This can be attributed to the use of simulations with a variable box shape and to a larger number of particles in each layer here, since both facilitate and speed-up equilibration. To conclude, we again find that the formation of the Col_+ phase in a system of crooked rods is due to finite-size effects.

4. Discussion and conclusions

In conclusions, our simulation results show that finite-size effects can be surprisingly significant in systems of rod-like particles forming layered structures such as smectic and crystal phases. In all the cases presented here, a Col_+ phase is formed at high pressures in systems with a small number of particle layers, but this phase becomes mechanically unstable for systems with a larger number of layers. These finite-size effects are quite

general as we find the formation of the Col_+ phase for a wide variety of systems, such as spherocylinders, top-shaped rods, cuboidal rods and crooked rods, and for Col_+ phases that are competing with a variety of thermodynamic phases such as smectic and crystal phases. As a consequence, it is difficult to predict the number of layers that is required to avoid these finite-size effects. For instance, we observed that $n=4$ particle layers were not always sufficient to circumvent these finite-size effects. But as a rule of thumb, we notice that the larger the particle anisotropy, the less severe the simulation artefacts, which is, perhaps, unexpected.

Our findings that all the simulated Col_+ phases that are reported in the literature so far in (freely rotating) single-component hard-particle systems are mechanically unstable, raises the question whether such a phase can be entropically stabilised at all in such systems. The answer to this question has interesting repercussions for our microscopic understanding of the phase behaviour of fd-virus suspensions, which show such a Col_+ phase. We wish to make two remarks here. First of all, the idea that only (oblate) disk-like particles can form (oblate) columnar phases and that only (prolate) rod-like particles can form (prolate) smectic phases is clearly wrong. Furthermore, the distinction between oblate versus prolate and disk-like versus rod-like is not always straightforward, as it is not always easy to predict if a particle behaves more like a rod or a plate [22,27]. For instance, systems of (biaxial) cuboids can show plate-like behaviour when they are more rod-like and vice versa [27], and their phase diagram can display prolate but also oblate smectic Sm_- phases [43]. It is therefore interesting to determine what the particle shape requirements are for the stabilisation of a Col_+ phase. It is well understood that polydisperse systems of rod-like particles can form a Col_+ phase [22,53,54]. Would it be possible to model the properties of length-polydisperse rods in a single-component system? The Col_+ phase was indeed observed in systems of rod-like particles with patchy attractions between the ends of the rods, i.e. sticky cylinders [55]. Such rods self-assemble in linear aggregates, whose flexibility depends on the binding energy. It is thus worthwhile to investigate if flexibility of purely repulsive rods could be the key factor for stabilising the Col_+ phase, a hypothesis that has been put forward for fd-virus suspensions [33,34]. However, recent simulations on semi-flexible rod-like particles [56], even though with aspect ratios much smaller than the experimental fd-virus particles [34], did not show any sign of a stable Col_+ phase. Another possibility might be that the Col_+ phase is stabilised by the chirality of the rods, but extensive simulation studies performed on hard helices did not report any evidence of a columnar phase [24,57]. In conclusion, the stabilisation of a Col_+

phase by entropy alone remains a puzzle that is still unresolved. More simulations are definitely required to unveil the microscopic origin of such a phase, but our results in this paper show that finite-size effects should be taken into account.

Acknowledgements

It is a great pleasure to contribute to this Special Issue of Molecular Physics in honour of Daan Frenkel on the occasion of his 70th birthday. M.D. first met Daan Frenkel when she applied for a studentship at the FOM Institute AMOLF in Amsterdam in the early 1990s. During that interview, M.D. was introduced by Daan Frenkel to the field of computer simulations. The greyscale movies of (what we now know a metastable columnar phase of) parallel hard spherocylinders that Jan Veerman presented to her made such a lasting impression that she did not hesitate when a Ph.D. position instead of a studentship was offered to her in Daan's group. As a consequence, M.D. had the privilege to be a Ph.D. student in the highly inspiring and thriving research group of Daan Frenkel. M.D. still benefits from the excellent scientific guidance that Daan Frenkel offered to her during her Ph.D. including his immense knowledge on a wide variety of topics, his deep insights and highly inspiring discussions. Daan's research, his pedagogical style of writing scientific papers and reviews, his lively presentations with a good sense of humour and, in particular, his book with the hand-drawn pictures, have been an unimaginable source of inspiration to her and others in the field. An important lesson that M.D. has learned from Daan is to calculate free energies to determine the phase behaviour. We offer our sincere apologies to Daan that we did not perform any free-energy calculations in this paper. M.D. thanks Daan for all the support she received from him over the years, but also for all the social activities such as the Daan weekends, dinner parties in Bussum and Cambridge, and the more recent annual dinners in Amsterdam with the 'old group of PhD students'. S.D. and M.C. also thank Daan Frenkel for his inspiring science: his pioneering simulations continue to have a strong influence on young researchers, his entertaining presentations motivate them and his textbook greatly contributes to their formation as computational physicists. It is with great pleasure that we congratulate Daan Frenkel with his 70th birthday and we wish him all the very best in the coming years.

Disclosure statement

No potential conflict of interest was reported by the authors.

Funding

S.D. and M.D. acknowledge financial support from Nederlandse organisatie voor Wetenschappelijk Onderzoek [NWO-ECHO grant]. M.C. and M.D. would like to acknowledge the financial support from the EU H2020-MSCA-ITN- 2015 project 'MULTIMAT' (Marie Skłodowska-Curie Innovative Training Networks) [project number: 676045].

References

- [1] P.G. de Gennes and J. Prost, *The Physics of Liquid Crystals* (Oxford University Press, Oxford, 1993).

- [2] G. Oster, *J. Gen. Physiol.* **33**, 445 (1950).
- [3] S. Fraden, G. Maret, D.J.D. Caspar, and R.B. Meyer, *Phys. Rev. Lett.* **63**, 2068 (1989).
- [4] Z. Dogic and S. Fraden, *Phys. Rev. Lett.* **78**, 2417 (1997).
- [5] Z. Dogic and S. Fraden, *Curr. Opin. Colloid Interface Sci.* **11**, 47 (2006).
- [6] F. Livolant and A. Leforestier, *Prog. Polym. Sci.* **21**, 1115 (1996).
- [7] Y. Maeda and S. Hachisu, *Colloids Surf.* **6**, 1 (1983).
- [8] H. Maeda and Y. Maeda, *Phys. Rev. Lett.* **90**, 018303 (2003).
- [9] M.P.B. van Bruggen, J.K.G. Dhont, and H.N.W. Lekkerkerker, *Macromolecules* **32**, 2256 (1999).
- [10] O. Pelletier, P. Davidson, C. Bourgeaux, and C. Livage, *Europhys. Lett.* **48**, 53 (1999).
- [11] A. Kuijk, A. van Blaaderen, and A. Imhof, *J. Am. Chem. Soc.* **133**, 2346 (2011).
- [12] A. Kuijk, D.V. Byelov, A.V. Petukhov, A. van Blaaderen, and A. Imhof, *Faraday Discuss.* **159**, 181 (2012).
- [13] L. Onsager, *Ann. N. Y. Acad. Sci.* **51**, 627 (1949).
- [14] D. Frenkel, B.M. Mulder, and J.P. McTague, *Phys. Rev. Lett.* **287**, 52 (1984).
- [15] D. Frenkel, H.N.W. Lekkerkerker, and A. Stroobants, *Nature* **332**, 822 (1988).
- [16] J.A.C. Veerman and D. Frenkel, *Phys. Rev. A* **45**, 5633 (1992).
- [17] D. Frenkel, *Phys. A* **263**, 26 (1999).
- [18] S. Torquato and Y. Jiao, *Nature* **460**, 876 (2009).
- [19] U. Agarwal and F.A. Escobedo, *Nat. Mater.* **10**, 230 (2011).
- [20] P.F. Damasceno, M. Engel, and S.C. Glotzer, *Science* **337**, 453 (2012).
- [21] L.J. Ellison, D.J. Michel, F. Barmes, and D.J. Cleaver, *Phys. Rev. Lett.* **97**, 237801 (2006).
- [22] L. Mederos, E. Velasco, and Y. Martinez-Raton, *J. Phys.* **26**, 463101 (2014).
- [23] C. Greco and A. Ferrarini, *Phys. Rev. Lett.* **115**, 147801 (2015).
- [24] H.B. Kolli, E. Frezza, G. Cinacchi, A. Ferrarini, A. Giacometti, T.S. Hudson, C. De Michele, and F. Sciortino, *Soft Matter* **10**, 8171 (2014).
- [25] M. Dijkstra, *Adv. Chem. Phys.* **156**, 35 (2015).
- [26] S. Dussi and M. Dijkstra, *Nature Comm.* **7**, 11175 (2016).
- [27] S. Dussi, N. Tasios, T. Drwenski, R. van Roij, and M. Dijkstra, preprint, arXiv:1801.07134 (2018).
- [28] Y. Xia, Y. Xiong, B. Lim, and S. Skrabalak, *Angew. Chem. Int. Ed.* **48**, 1 (2009).
- [29] J. Gong, G. Li, and Z. Tang, *Nano Today* **7**, 564 (2012).
- [30] L. Zhang, W. Niu, and G. Xu, *Nano Today* **7**, 586 (2012).
- [31] H.E. Bakker, S. Dussi, B.L. Droste, T.H. Besseling, C.L. Kennedy, E.I. Wiegant, B. Liu, A. Imhof, M. Dijkstra, and A. van Blaaderen, *Soft Matter* **12**, 9238 (2016).
- [32] E. Grelet and S. Fraden, *Phys. Rev. Lett.* **90**, 198302 (2003).
- [33] E. Grelet, *Phys. Rev. X* **4**, 021053 (2014).
- [34] E. Grelet and R. Rana, *Soft Matter* **12**, 4621 (2016).
- [35] M. Marechal, A. Patti, M. Dennison, and M. Dijkstra, *Phys. Rev. Lett.* **108**, 206101 (2012).
- [36] F.M. van der Kooij, K. Kassapidou, and H.N.W. Lekkerkerker, *Nature* **406**, 868 (2000).
- [37] A. Stroobants, H.N.W. Lekkerkerker, and D. Frenkel, *Phys. Rev. A* **36**, 2929 (1987).
- [38] J.A.C. Veerman and D. Frenkel, *Phys. Rev. A* **43**, 4334 (1991).
- [39] P. Bolhuis and D. Frenkel, *J. Chem. Phys.* **106**, 666 (1997).
- [40] S.C. McGrother, D.C. Williamson, and G. Jackson, *J. Chem. Phys.* **104**, 6755 (1996).
- [41] Y. Lansac, P.K. Maiti, N.A. Clark, and M.A. Glaser, *Phys. Rev. E* **67**, 011703 (2003).
- [42] D. de las Heras, S. Varga, and F.J. Vesely, *J. Chem. Phys.* **134**, 214902 (2011).
- [43] A. Cuetos, M. Dennison, A. Masters, and A. Patti, *Soft Matter* **13**, 4720 (2017).
- [44] P. Datskos, J. Chen, and J. Sharma, *RSC Adv.* **4**, 2291 (2014).
- [45] Y. Yang, G. Chen, L.J. Martinez, H. Yu, K. Liu, and Z. Nie, *J. Am. Chem. Soc.* **138**, 68 (2016).
- [46] D. Frenkel and B. Smit, *Understanding Molecular Simulation: From Algorithms to Applications* (Academic Press, San Diego, 2002).
- [47] C. Vega and S. Lago, *Comput. Chem.* **18**, 55 (1994).
- [48] GAMMA Research Group at the University of North Carolina, RAPID – Robust and Accurate Polygon Interference Detection. (<http://gamma.cs.unc.edu/OBB/1997>).
- [49] M.P. Allen and D.J. Tildesley, *Computer Simulation of Liquids* (Clarendon Press, Oxford, 1989).
- [50] L. Fillion, M. Marechal, B. van Oorschot, D. Pelt, F. Smalenburg, and M. Dijkstra, *Phys. Rev. Lett.* **103**, 188302 (2009).
- [51] B.S. John, C. Juhlin, and F.A. Escobedo, *J. Chem. Phys.* **128**, 044909 (2008).
- [52] B.S. John and F.A. Escobedo, *J. Phys. Chem. B* **109**, 23008 (2005).
- [53] M.A. Bates and D. Frenkel, *J. Chem. Phys.* **109**, 6193 (1998).
- [54] S. Varga, E. Velasco, L. Mederos, and F.J. Vesely, *Mol. Phys.* **107**, 2481 (2009).
- [55] T. Kuriabova, M.D. Betterton, and M.A. Glaser, *J. Mater. Chem.* **20**, 10366 (2010).
- [56] B. de Braaf, M.O. Menegon, S. Paquay, and P. van der Schoot, *J. Chem. Phys.* **147**, 244901 (2017).
- [57] H.B. Kolli, G. Cinacchi, A. Ferrarini, and A. Giacometti, *Faraday Discuss.* **186**, 171 (2016).